RSC Advances

PAPER

View Article Online
View Journal | View Issue

Cite this: *RSC Adv.*, 2021, **11**, 29407

Antioxidant and anti-aging potential of a peptide formulation (Gal_2–Pep) conjugated with gallic acid†

Hoomin Lee, ‡[ad] Kwanwoo Kim,‡[ad] Cheolwoo Oh,[ad] Chi-Hu Park,[b] Sheik Aliya,[ad] Hyoung-Shik Kim,[b] Vivek K. Bajpai*[c] and Yun Suk Huh *[ad]

Skin is highly vulnerable to premature aging due to external stress, therefore, in this study, a peptide formulation, (galloyl)$_2$–KTPPTTP (Gal_2–Pep) was synthesized by combining TPPTTP peptide, and gallic acid (GA). All peptides were synthesized on 2-chlorotrityl chloride resin using solid-phase peptide synthesis (SPPS), and analyzed on an electrospray ionization (ESI)/quadrupole-time-of-flight (Q-TOF) tandem mass spectroscopy (MS) system. Initially, Gal_2–Pep showed no toxicity below the concentration 100 μM with cell survival rate of 88% for keratinocytes and fibroblasts. The reactive oxygen species (ROS) scavenging activity of Gal_2–Pep was more stable compared to GA alone; and after four weeks at room temperature, its ROS scavenging activity remained higher than 50%. Moreover, the peptide formulation, Gal_2–Pep also exhibited elastase inhibitory effect in CCD-1064Sk fibroblast cells. Based on the results of RT-qPCR, it was proved in this study that Gal_2–Pep increased the expression of PGC-1α to prevent oxidative stress, and validated its potential as an anti-aging agent through increasing the expression of type I collagen and by decreasing the expression of matrix metalloproteinase-1 (MMP1). The findings obtained reinforce the suggestion that the peptide formulation synthesized in this study could be used as a natural antioxidant and anti-aging agent for its cosmetic applications.

Received 1st May 2021
Accepted 24th August 2021

DOI: 10.1039/d1ra03421a

rsc.li/rsc-advances

1. Introduction

Skin aging occurs as a result of the gradual decrease in and eventual halting of the cell division of keratinocytes and fibroblasts within the skin. Wrinkles on the skin develop as the number of cells decreases, with the resulting denaturation of the extracellular matrix leading to dryness and a loss of elasticity in the skin.[1] Damage to intracellular mitochondrial DNA and a reduction in the rate of protein synthesis also occur during the skin aging process.[2] Skin aging has two main pathways, intrinsic and extrinsic, with ultraviolet (UV) exposure a major driver of extrinsic aging. The UV light reacts with major components of the skin, including lipids, proteins, and nucleic acids, to produce reactive oxygen species (ROS) that lead to cell death.[3–5] Excessive ROS levels also lead to the cleavage and abnormal binding of collagen or elastin chains and promote the expression of matrix metalloproteinases (MMPs), such as MMP-1, that break down collagen, leading to the wrinkling of the skin and accelerating skin aging.[6,7] Therefore, antioxidant therapy to remove ROS and to activate mitochondrial potential has the merits to protect the skin from aging.

In addition to ROS, elastase has a significant role in the loss of skin elasticity, which breaks down elastin, an important protein of extracellular matrix.[8] Elastin, due to its significant elastic recoil characteristics, provide elasticity to the skin, whereas elastase has the ability to cleave elastin and other proteins.[8] Therefore, inhibition of elastase enzyme could be a pivotal strategy for skin sagging *via* preventing the loss of skin elasticity.

In this study, we designed a new material that combines the peroxisome proliferator-activated receptor gamma coactivator 1-alpha (PGC-1α)-derived peptide TPPTTP and gallic acid (GA) for use in anti-aging cosmetics. GA is a phytochemical found in various fruits and vegetables, including grapes, tomatoes, and green tea, that is known to have high antioxidant and antibacterial effects.[9] Though GA is used in the cosmetics and food industries because of these beneficial effects, its formulation tends to be unstable.[10] We thus developed (galloyl)$_2$–KTPPTTP (Gal_2–Pep) in order to increase the stability of GA by binding it to the PGC-1α-derived peptide TTPTTP.

[a]*Department of Biological Sciences and Bioengineering, Nano Bio High-Tech Materials Research Center, Inha University, Incheon 22212, Republic of Korea. E-mail: yunsuk.huh@inha.ac.kr*

[b]*Natural Bioactive & Anticancer Research Institute, YEPBio Co., Ltd., 282 Hagui-ro, Anyang-city, Gyeonggi-do, Republic of Korea*

[c]*Department of Energy and Materials Engineering, Dongguk University, 30 Pildong-ro 1-gil, Seoul 04620, Republic of Korea. E-mail: vbiotech04@gmail.com*

[d]*Department of Biosystems and Bioengineering, Inha University, Incheon 22212, Republic of Korea*

† Electronic supplementary information (ESI) available. See DOI: 10.1039/d1ra03421a

‡ These authors contributed equally to this work.

In this study, we synthesized a $(galloyl)_2$–KTPPTTP (Gal_2–Pep) peptide formulation in conjugation with gallic acid and confirmed its potential as an antioxidant and antiaging agent.

2. Materials and methods

2.1. Materials

Dulbecco's Modified Eagle's Medium (DMEM), penicillin/streptomycin, fetal bovine serum (FBS), phosphate-buffered saline (PBS), and trypsin were purchased from Gibco (Carlsbad, CA). Hydroxybenzotriazole (HOBt), diisoproylcarbodiimide (DIC), 1,8-diazabicyclo[5.4.0]undec-7-en (DBU), *N*,*N*-diisopropylethylamine (DIEA), gallic acid and *N*-succinyl-tri-alanyl-*p*-nitroanilide were obtained from Sigma-Aldrich (St. Louis, MO). L-Form amino acids (Fmoc-Lys (Boc)–OH, Fmoc-Thr (*t*Bu)–OH, and Fmoc-Pro–OH) were purchased from Bead-Tech (Seoul, Korea).

2.2. Synthesis of peptides and gallic acid-coupled peptides

All peptides were synthesized on 2-chlorotrityl chloride resin (200 μmol scale, substitution value = 1.46 mmol g^{-1}) using HOBt–DIC mediated solid-phase peptide synthesis (SPPS). Peptide synthesis using the SPPS method was carried out with slight modifications referring to previous studies.[11–13] The 2-chlorotrityl chloride (CTC) resin was swelled in dichloromethane (DCM, 8 mL) for 30 min. The resin was washed with dimethylformamide (DMF). All reactions were carried out at room temperature. Fmoc protected amino acid derivatives (2 equivalent (equiv.), for first attached amino acid or 5 equiv., for the other amino acids) were coupled with either DIEA (5 equiv., for first attached amino acid) or HOBt/DIC (6 equiv./5 equiv.) in DMF after performing deprotection of Fmoc using 2% (v/v) DBU in DMF (2 times, 2 min a time, 8 mL). And all steps were washed 5 times with DMF. Final gallic acid was coupled with lysine attached peptides. After the coupling of the gallic acid, the resin was filtered, washed, and dried under high vacuum. The cleavage solution (TFA: deionized [DI] water: TIS = 95 : 2.5 : 2.5, v/v/v%) was treated for 2 h to obtain the crude peptides. The crude peptides were precipitated and washed three times with cold diethyl ether.

Analytical reverse-phase high-performance liquid chromatography (RP-HPLC) was conducted on a Waters 2695 Separations Module with a Capcell Pak C18 column (4.6 mm × 250 mm, 5 μm, Shiseido). The mobile phase consisted of 0.05% TFA in H_2O (mobile phase A) and 0.05% TFA in acetonitrile (mobile phase B). Elution was achieved by employing a linear gradient for mobile phase B of 5% to 65% over 30 min at a flow rate of 1.0 mL min^{-1}. The peptide peaks were detected at a wavelength of 230 nm.

Semi-preparative RP-HPLC was conducted on a Waters HPLC system (Pump 600E, Detector UV-484) with a Gemini RP-C18 column (21.2 mm × 250 mm, 5 μm, Phenomenex). The mobile phase consisted of 0.05% TFA in H_2O (mobile phase A) and 0.05% TFA in acetonitrile (mobile phase B). Elution was achieved by employing a linear gradient for mobile phase B of 7% to 22% over 15 min at a flow rate of 10 mL min^{-1}. The peptide peaks were detected spectrophotometrically at a wavelength of 230 nm.

The synthesized peptides were dissolved in 5% formic acid in water and analyzed on an electrospray ionization (ESI)/quadrupole-time-of-flight (Q-TOF) tandem mass spectroscopy (MS) system (TripleTOF6600, ABSciex, Foster City, CA). The samples were injected into the Q-TOF system equipped with a nano-spray source at a flow rate of 1 μL min^{-1}. The ESI ion source parameters were as follows: an ion spray voltage of 1.5 kV, curtain gas at 10 psi, and sheath gas at 5 psi. The spectra in full-scan mode and MS/MS were collected in the range of m/z 100–1200 Da at an accumulation time of 25 ms per spectrum. The collision energy was ramped from 10 to 80. The resultant data were acquired using Analyst TF software and automatically assigned by centroid 80% with a minimum peak, noise reduction of 10%, medium deisotoping with a 3% threshold, no noise reduction, and no smoothing. The synthesized peptides were identified with a mass tolerance of ± 0.05 Da and manually sequenced using an MS/MS tolerance of ± 0.01 Da.

2.3. Cell cultures and viability assays

Human, adult, low calcium, high temperature (HaCaT) cells and CCD-1064Sk (normal human skin fibroblast) cells were cultured in DMEM with 10% FBS and 1% penicillin/streptomycin. The cells were incubated at 37 °C in a humidified air chamber with 5% CO_2.

For the viability assays, cell counting kit-8 (CCK-8, Dojindo Co. Ltd. Beijing, China) was used. HaCaT and CCD-1064Sk cells were seeded in 96-well microplates (5×10^3 cells per well) and incubated at 37 °C in 5% CO_2 for 24 h. The cultures were then exposed to different concentrations of the synthesized peptides or GA and incubated at 37 °C in 5% CO_2 for 24 h. Cell viability was subsequently measured using a CCK-8 following the manufacturer's guidelines.

2.4. Determination of antioxidant activity

2.4.1. DPPH assay. The antioxidant activity of the synthesized peptides and GA was evaluated individually using DPPH assay. DPPH assay were performed following a previously reported methodology with minor modification.[12,14–16] First, a 0.12 mg mL^{-1} DPPH solution was prepared in methanol, then 100 μL of DPPH solution and 100 μL of the synthesized peptides or GA were mixed at different concentrations (0.1 mM, 0.05 mM, 0.01 mM, and 1 μM) in 96-well microplates. In an orbital shaking incubator, the mixtures were reacted for 30 min at 37 °C and 100 rpm without light. The absorbance was then measured at 517 nm and the antioxidant capacity was calculated.

2.4.2. ROS scavenging activity. Intracellular ROS scavenging activity was evaluated using a 2′,7′-dichlorofluorescin diacetate kit (DCF-DA, Abcam, USA). HaCaT cells were seeded in 96-well microplates (5×10^3 cells per well) and incubated at 37 °C for 24 h. After incubation, the cultures were exposed to the synthesized peptides or GA (100 μM) and incubated at 37 °C for 24 h. The cells were then exposed to a 10 μM DCF-DA solution and incubated for 30 min. After incubation, the solution was washed with PBS. The cells were analyzed using a microplate reader at excitation and emission wavelengths of 485 nm and 530 nm, respectively.

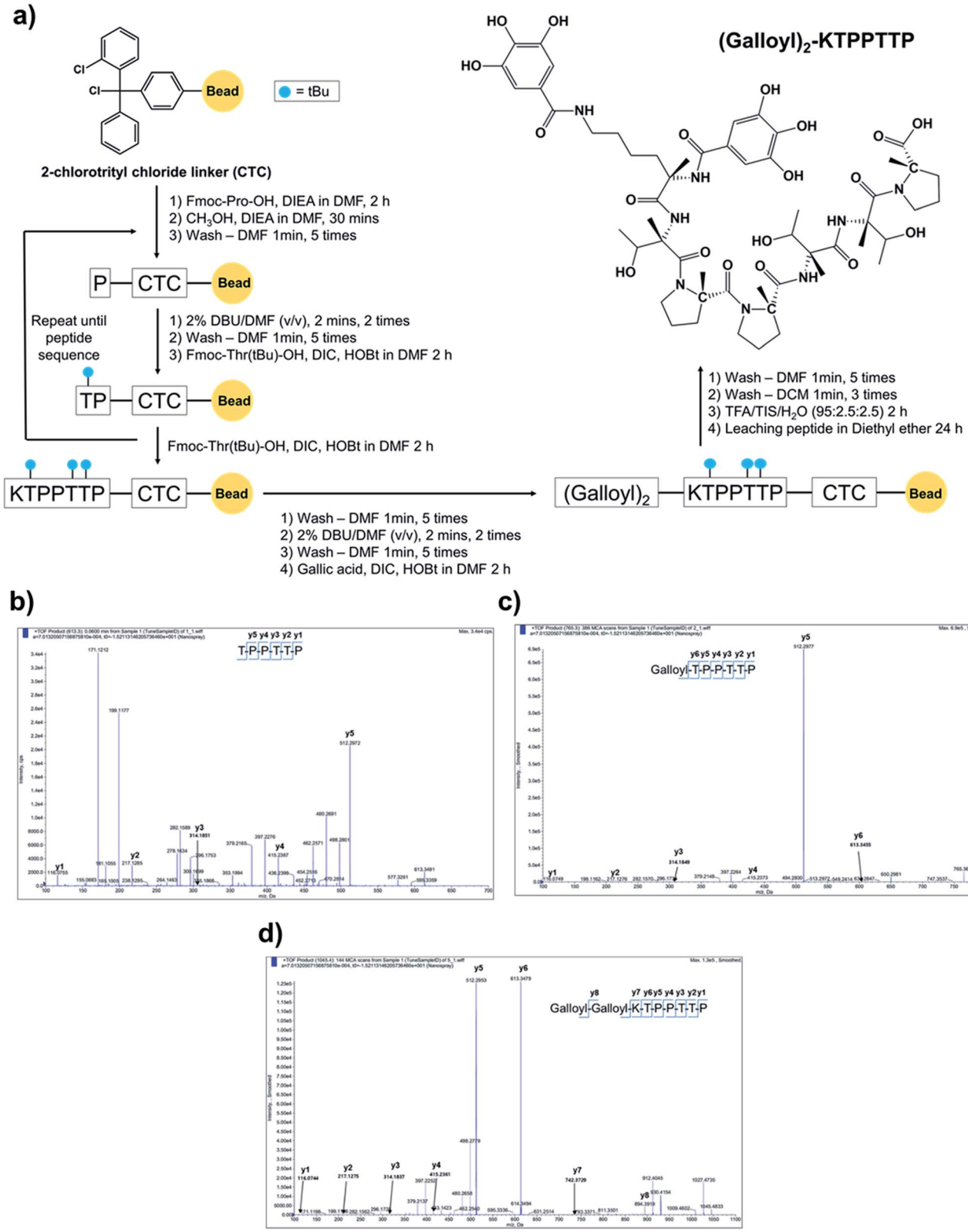

Fig. 1 Synthetic step and sequence confirmation of peptides using quadrupole-time of flight (Q-TOF) mass spectrometry: (a) detailed synthetic procedure (b) TPPTTP, (c) galloyl–TPPTTP, and (d) $(galloyl)_2$–KTPPTTP.

2.5. Mitochondrial membrane potential assay

JC-1 dye (Thermo Fisher, USA) was used for the mitochondrial membrane potential (MmP) assay. CCD-1064Sk and HaCaT cells were seeded in 96-well microplates (5×10^3 cells per well) and incubated at 37 °C and in 5% CO_2 for 24 h. After incubation, the cultures were exposed to different concentrations of the synthesized peptides and incubated at 37 °C in 5% CO_2 for 24 h. JC-1 dye was added to the CCD-1064Sk and HaCaT cells to produce a final concentration of 10 μM. After 10 min of incubation, the cells were washed twice with 37 °C PBS. Green and red fluorescences were measured using a Varioskan LUX Multimode Microplate Reader (ThermoFisher, USA) at an excitation (λ_{Ex})/emission (λ_{Em}) of 475/530 nm and an $\lambda_{Ex}/\lambda_{Em}$ of 475/590 nm, respectively.

2.6. Elastase inhibitory activity assay

CCD-1064Sk cells were seeded in 6-well plates and incubated at 37 °C in 5% CO_2 for 24 h. The cultures were then exposed to concentration of 100 μM of the synthesized peptides or GA and incubated at 37 °C in 5% CO_2 for 24 h. Cells were washed with dPBS twice and we collected each cell using cell scraper. After adding 0.2 M Tris–HCl (pH 8.0) with 0.1% Triton-X to the collected cells, cells were homogenized by ultrasonicator. The homogenized solution was centrifuged for 20 min at 3000 rpm and 4 °C. Then, after taking the supernatant, protein quantification was performed using BCA protein assay. Protein for each sample was dispensed at the final concentration of 100 μg mL^{-1}, and *N*-succinyl-tri-alanyl-*p*-nitroanilide was added at the final concentration of 1.6 mM, and reacted at 36 °C for 1 h. Then, the absorbance was measured at 405 nm using a microplate reader.

2.7. RT-qPCR

The mRNA levels of anti-aging markers in CCK-1064Sk cells were assessed using RT-qPCR. Total RNA was collected using TRIzol reagent (Life Technologies, Carlsbad, CA) and reverse-transcribed using the PrimeScript RT reagent kit (Takara Bio Inc., Kusatsu, Japan). A CFX96 system (Bio-Rad Laboratories, Hercules, CA) and iQ SYBR Green Supermix (Bio-Rad Laboratories) were used for RT-qPCR. β-Actin was used to normalize the mRNA levels of type I collagen, MMP-1, and PGC-1α.

2.8. Statistical analysis

The data are presented as the mean ± standard deviation from three independent measurements and analyzed using Student's *t*-tests, with a $p < 0.05$ considered to be a significant difference.

3. Results and discussion

3.1. Synthesis and conjugation of gallic acid with peptide

The synthesized peptides TPPTTP, galloyl–TPPTTP (Gal–Pep), and Gal_2–Pep were obtained and purified using semi-preparative RP-HPLC. Fig. 1a and Scheme 1 show conjugation strategy of gallic acid with KTPPTTP as Gal_2–Pep. In the SPPS method, the

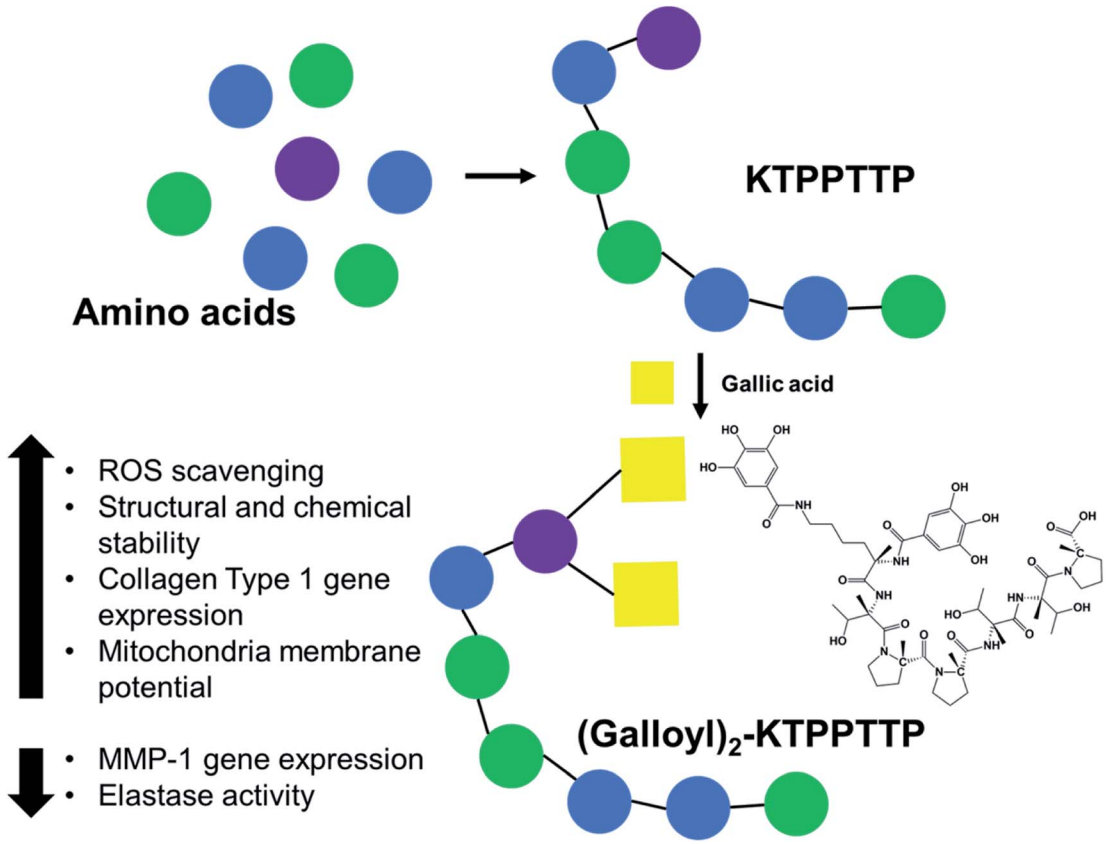

Scheme 1 Conjugation strategies of gallic acid with peptide as an anti-oxidant and anti-aging agent of (galloyl)$_2$–KTPPTTP.

impurities generated during peptide synthesis usually include side-reacted peptides, amino acid protecting groups, and solvents used for synthesis and purification. The HOBt used in peptide synthesis is known to inhibit the racemization and improve the efficiency of peptide synthesis.[17–19] In order to remove amino acid protecting groups and solvents used for synthesis, we performed washing several times using solvents such as DMF and DCM during the peptide synthesis process. Even after the last washing step, impurities including amino acid protecting groups are still present in trace amounts. In order to meet the peptide purity of more than 90% reported by several researchers,[20–22] semi-prep HPLC was performed as a polishing step to obtain the final peptide of 99.2% purity as a result of HPLC analysis (see Fig. S1†). The purified peptide product was analyzed using Q-TOF to reconfirm their successful synthesis (Fig. 1b–d).

3.2. Cell viability assays

To investigate the cytotoxicity of the synthesized peptides, HaCaT and human dermal fibroblast cells were treated with various concentrations of GA, TPPTTP, Gal–Pep, and Gal_2–Pep for 24 h and analyzed using CCK-8 assays. It was confirmed that the synthesized peptides had no toxic effect on the treated cells, with a cell viability of at least 88% for all samples and all the concentrations tested (Fig. 2a and b), indicating that TPPTTP, Gal–Pep, and Gal_2–Pep are suitable for use in cosmetics applications. Additionally, it was confirmed by MTT, LDH and Griess reagent assay that the final peptide did not cause toxicity in HA and F and inflammatory response in raw 264.7. (Fig. S2–S4†).

3.3. Antioxidant activity of synthesized peptides

The mechanisms involved in skin aging include ROS activity, mitochondrial DNA mutations, the shortening of telomeres, and hormonal changes, particularly in women.[23] ROS act as cell signaling molecules for many cellular processes, such as differentiation and proliferation.[24] However, excessive ROS can lead to the cleavage and abnormal binding of collagen and elastin chains and increase the expression of MMP-1, an enzyme that breaks down collagen, thus accelerating aging and cell apoptosis. Therefore, it is important to remove ROS from skin cells to promote anti-aging effects. In this study, we confirmed the antioxidant activity of the synthesized peptides through DPPH and DCF-DA assays.

Fig. 3a presents the results of the radical scavenging activity of the synthesized peptides as measured using DPPH assay. TPPTTP had no radical scavenging activity at any concentration, while GA, Gal–Pep, and Gal_2–Pep exhibited higher radical scavenging activity in a concentration-dependent manner. In

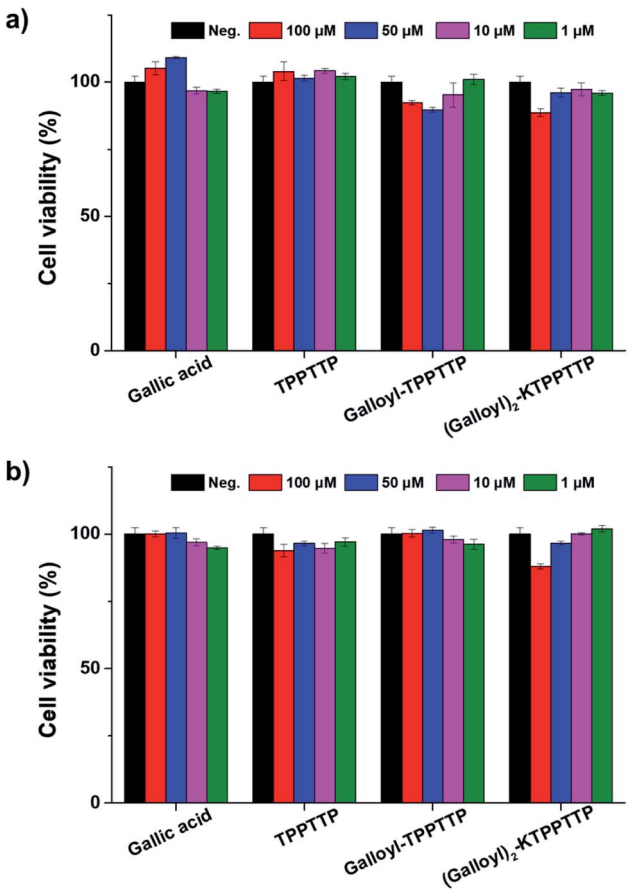

Fig. 2 Cell viability of (a) HaCaT cells and (b) dermal fibroblasts with gallic acid and peptide treatment.

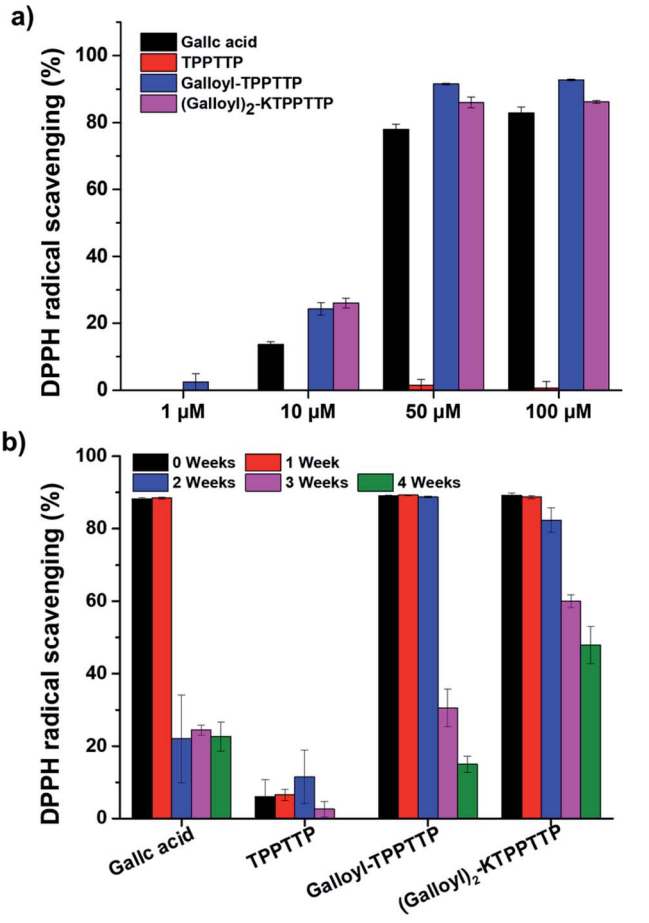

Fig. 3 (a) Effect of gallic acid and peptides on radical scavenging activity using DPPH assays. (b) Long-term stability testing using DPPH assays at a concentration of 100 μM.

particular, Gal_2–Pep demonstrated the most effective antioxidant activity; at a concentration of 10 μM, GA, Gal–Pep, and Gal_2–Pep had radical scavenging activity of 13.6%, 24.23%, and 26.0%, respectively. This indicates that the binding of TPPTTP to GA does not inhibit the radical scavenging activity. Fig. 3b confirms the stability of the samples as confirmed by assessing their radical scavenging activity when stored at room temperature. GA retained its radical scavenging activity for up to one week but, after two weeks, this activity decreased by more than 60%. On the other hand, Gal–Pep and Gal_2–Pep maintained their scavenging activity for over two weeks. In particular, Gal_2–Pep had a radical scavenging activity of 50% even in its fourth week. These results suggest that binding GA to TPPTTP stabilizes its radical scavenging activity. Some studies have shown that ascorbic acid is stabilized by binding it with peptides.[12,25] We believe that GA may be stabilized by binding it with a peptide in the same way.

The antioxidant effect of the peptides was also tested using DCF-DA assays in the presence of intracellular oxidative stress induced by H_2O_2 (Fig. 4). After 24 h of treating the samples on the cells at concentration of 100 μM, DCF-DA was loaded onto the cells, and the cells were then treated with H_2O_2 for 30 min and the fluorescence intensity of DCF was observed at an excitation wavelength of 485 nm and an emission wavelength of 535 nm. Cells subjected to oxidative stress with 1 mM H_2O_2 exhibited fluorescence intensity that was more than three times higher than the negative control; however, Gal_2–Pep treatment produced a fluorescence that was only 67% of that produced by cells treated with H_2O_2 only. In the presence of TPPTTP, which did not exhibit radical scavenging activity (Fig. 3a), the ROS stress caused by H_2O_2 was reduced by about 20%, supporting previous research that has reported that TPPTTP decreases ROS levels in cells.[24] When the cells were treated with GA only, there was no significant change in ROS levels. Taken together, these results suggest that Gal_2–Pep, which combines two GA molecules with a peptide, is a stable and effective antioxidant.

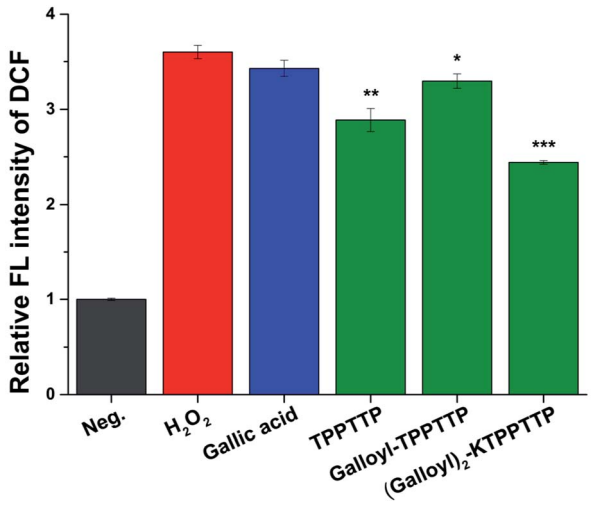

Fig. 4 Intracellular antioxidant activity assays using DCF-DA at gallic acid and peptide concentrations of 100 μM. After 24 hours of treatment, H_2O_2 was added and incubated for 30 minutes, followed by measurement of DCF fluorescence intensity. Asterisks indicate statistically significant differences (*p < 0.05, **p < 0.005, ***p < 0.001).

3.4. Effect of synthesized peptides on the mitochondria membrane potential

In this study, JC-1 dye was used to investigate the effect of the synthesized peptides on the MmP ($\Delta\Psi m$). The MmP acts as an important parameter for mitochondrial function and is known to be associated with several diseases such as Alzheimer's and Huntington's disease.[26] JC-1 dye produces a redshift from green emissions by accumulating in mitochondria and forming J-aggregates.

After treating the HaCaT and fibroblast cells with the synthesized peptides for 24 h, the cells were exposed to JC-1 dye for 10 min, and then the fluorescence intensity was measured using a microplate reader (green $\lambda_{Ex} = 475$ nm and $\lambda_{Em} = 530$ nm, red $\lambda_{Ex} = 475$ nm and $\lambda_{Em} = 590$ nm). The ratio of the red to green fluorescence was expressed as the fold-change compared to the negative control (Fig. 5). HaCaT cells treated with GA and the peptide independently did not exhibit any significant change compared to the negative control group, while Gal_2–Pep exhibited a significant difference, increasing 1.45-fold compared to the control. The fibroblast cells treated with Gal_2–Pep also significantly increased 1.12-fold compared to the negative control. The increase in MmP with Gal_2–Pep treatment clearly indicates that Gal_2–Pep is a biomolecule that can be employed in anti-aging cosmetics.

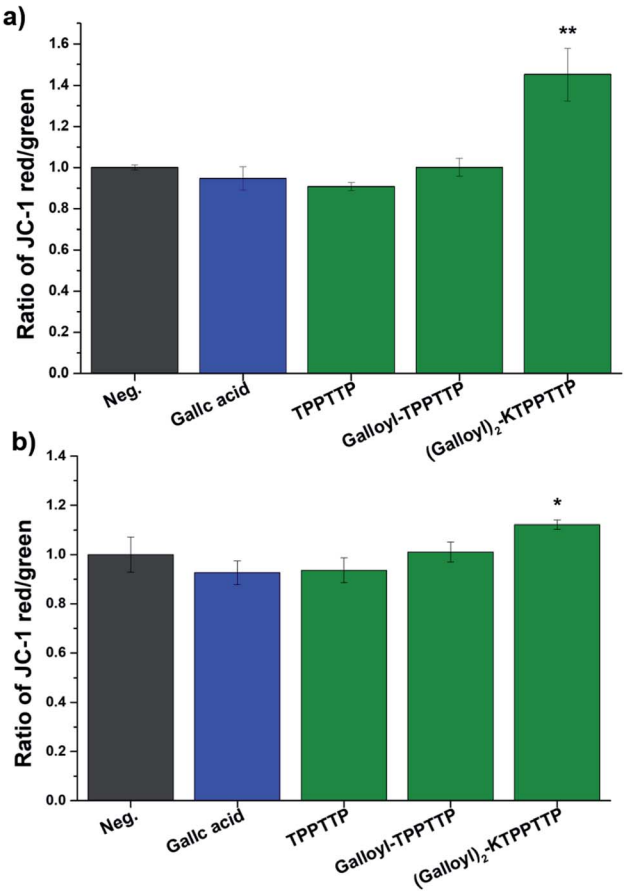

Fig. 5 Measurement of the mitochondrial membrane potential using JC-1 dye in (a) HaCaT cells and (b) dermal fibroblasts. Asterisks indicate statistically significant differences (*p < 0.05, **p < 0.005, ***p < 0.001).

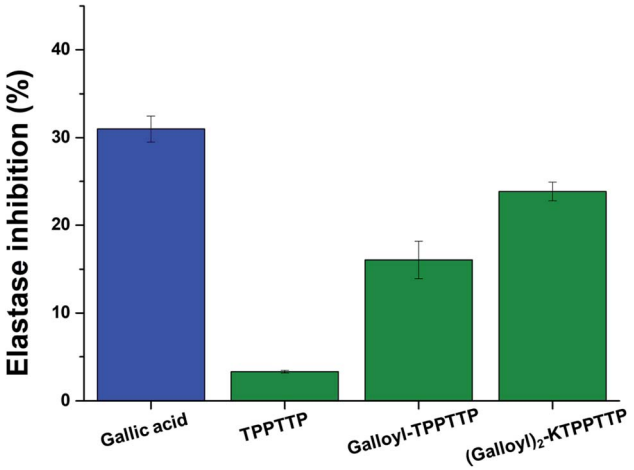

Fig. 6 Measurement of the elastase activity in dermal fibroblasts at gallic acid and peptide concentrations of 100 μM. Asterisks indicate statistically significant differences (*$p < 0.05$, **$p < 0.005$, ***$p < 0.001$).

3.5. Elastase inhibitory activity

Elastase promotes skin aging by breaking down collagen or elastin in the skin, so it can prevent skin aging by inhibiting elastase.[27] Fig. 6 shows elastase activity in CCD-1064Sk cells treated with each sample. TPPTTP has rare effect on elastase inhibition. However, treatment with gallic acid, Gal–Pep, and Gal_2–Pep showed elastase activity by 69%, 84% and 76%, respectively. Gal_2–Pep inhibited elastase by 7% less than that of GA. However, when considering the results of measurement of antioxidant effect, long-term stability, and mitochondrial membrane potential, Gal_2–Pep was more effective than GA as an anti-aging agent.

3.6. Expression of type I collagen, MMP-1, and PGC-1α genes

Fig. 7 shows RT-qPCR data of type I collagen, MMP-1, and PGC-1α gene expression. Type I collagen, a major component of the collagen family found within the skin, decreases as aging progresses.[28] When Gal_2–Pep was used to treat fibroblasts for 8 h and 24 h, the expression of type I collagen increased

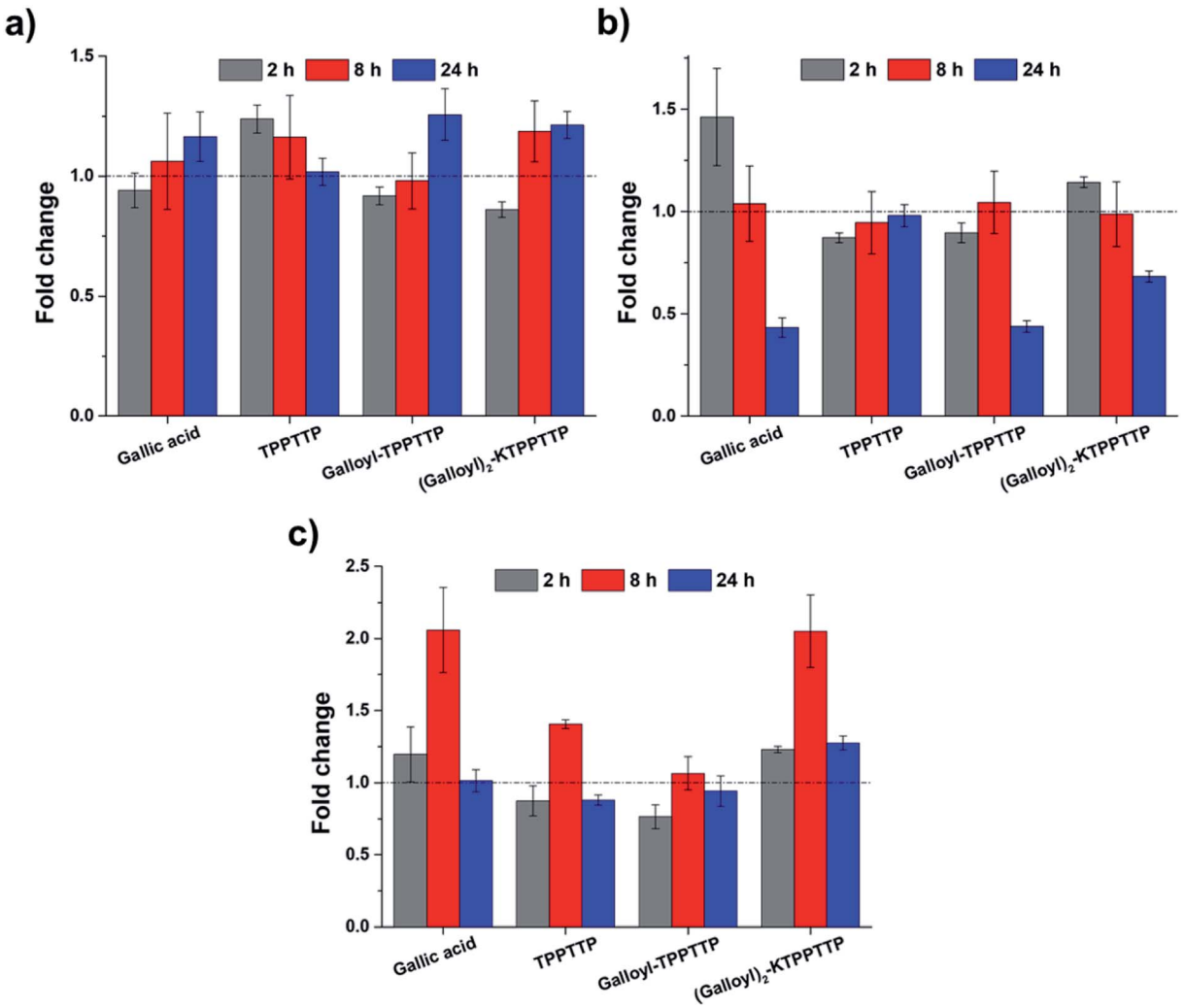

Fig. 7 Gene expression analysis in dermal fibroblasts using RT-qPCR: (a) type I collagen, (b) MMP-1, and (c) PGC-1α.

approximately 1.19- and 1.21-fold, respectively. With GA and Gal–Pep, there was no significant change after 2 h and 8 h, but type I collagen expression increased 1.16- and 1.26-fold after 24 h, respectively. With TTPTTP treatment, however, expression increased by 1.24-fold in the first 2 h and then gradually decreased. After 24 h, the expression level was similar to that of the negative control (Fig. 7a). For MMP-1, expression levels of 0.43, 0.44, and 0.68-fold were observed after 24 h with GA, Gal–Pep, and Gal_2–Pep treatment, respectively. In addition, the expression levels with GA treatment increased by 1.46-fold after 2 h. With TPPTTP, MMP-1 expression decreased 0.87-fold after 2 h, but subsequently became similar to that of the negative control. Overall, restoring collagen levels, which otherwise decreases with aging, helps to improve wrinkles.[28]

The expression of PGC-1α was highest after 8 h for all treatments, with expression rates for GA, TPPTTP, Gal–Pep, and Gal_2–Pep increasing 2.06-, 1.41-, 1.07-, and 2.05-fold, respectively. However, unlike the other treatments, Gal_2–Pep increased PGC-1α expression 1.27-fold after 24 h. PGC-1α regulates the synthesis and antioxidant effects of mitochondria and is reported to decrease with aging.[29–32] Therefore, Gal_2–Pep has the potential be used as an effective antioxidant that can effectively protect against ROS.

Taken all together, Gal_2–Pep increased the expression of PGC-1α and collagen compared to the effects of GA and TPPTTP alone, while the expression of MMP-1 tended to decrease, thus illustrating its potential for use in anti-aging cosmetics.

4. Conclusion

In this study, Gal_2–Pep, which was developed by combining GA and the peptide TPPTTP, which exhibited excellent antioxidant activity and mitochondrial activation in skin cells. The cell viability results clearly indicated that Gal_2–Pep has no cytotoxic effect on skin cells. Gal_2–Pep also demonstrated dose-dependent antioxidant and free radical scavenging activity, with ROS scavenging activity over 50% even after storage for four weeks at room temperature. It also positively influenced the MmP and increased the expression of PGC-1α, which regulates mitochondrial synthesis and has an antioxidant effect by eliminating free radicals within the skin. Gal_2–Pep also increased the expression of type I collagen and decreased elastase activity and the expression of MMP-1, proving that it holds promise for use in anti-aging cosmetics.

Conflicts of interest

There are no conflicts to declare.

Acknowledgements

This study was supported by a grant of the Korea Industrial Complex Corp. (KICOX, NTIS No. 1415165722) and Inha University Research Grant.

References

1 P. Brenneisen, H. Sies and K. Scharffetter-Kochanek, *Ann. N. Y. Acad. Sci.*, 2002, **973**, 31–43.
2 A. Trifunovic, A. Wredenberg, M. Falkenberg, J. N. Spelbrink, A. T. Rovio, C. E. Bruder, M. Bohlooly-Y, S. Gldlöf, A. Oldfors, R. Wibom, J. Törnell, H. T. Jacobs and N. G. Larsson, *Nature*, 2004, **429**, 417–423.
3 S. B. Khan, C. S. Kong, J. A. Kim and S. K. Kim, *Biotechnol. Bioprocess Eng.*, 2010, **15**, 191–198.
4 H.-J. Kim, K.-W. Kim, B.-P. Yu and H.-Y. Chung, *Free Radical Biol. Med.*, 2000, **28**, 683–692.
5 M. Erden Inal, A. Kahraman and T. Köken, *Clin. Exp. Dermatol.*, 2001, **26**, 536–539.
6 H. S. Jin, S. Y. Park, J. Y. Kim, J. E. Lee, H. S. Lee, N. J. Kang and D. W. Lee, *Biotechnol. Bioprocess Eng.*, 2019, **24**, 240–249.
7 H. Masaki, *J. Dermatol. Sci.*, 2010, **58**, 85–90.
8 T. S. A. Thring, P. Hili and D. P. Naughton, *BMC Complementary Altern. Med.*, 2009, **9**, 27.
9 L. Quiles-Carrillo, S. Montava-Jordà, T. Boronat, C. Sammon, R. Balart and S. Torres-Giner, *Polymers*, 2019, **12**, 31.
10 D. H. Park, D. H. Jung, S. J. Kim, S. H. Kim and K. M. Park, *BMC Biochem.*, 2014, **15**, 4–10.
11 Y. J. Cheng, G. F. Luo, J. Y. Zhu, X. D. Xu, X. Zeng, D. B. Cheng, Y. M. Li, Y. Wu, X. Z. Zhang, R. X. Zhuo and F. He, *ACS Appl. Mater. Interfaces*, 2015, **7**, 9078–9087.
12 H. Lee, A. T. E. Vilian, J. Y. Kim, M. H. Chun, J. S. Suh, H. H. Seo, S. H. Cho, I. S. Shin, S. J. Kim, S. H. Park, Y.-K. Han, J. H. Lee and Y. S. Huh, *RSC Adv.*, 2017, (48), 30205–30213.
13 Y. Kong, C. Xu, Z. L. He, Q. M. Zhou, J. Bin Wang, Z. Y. Li and X. Ming, *Peptides*, 2014, **53**, 70–78.
14 H. Kim, J. S. Kim, Y. G. Kim, Y. Jeong, J. E. Kim, N. S. Paek and C. H. Kang, *Biotechnol. Bioprocess Eng.*, 2020, **25**, 421–430.
15 M. A. Frezzini, F. Castellani, N. De Francesco, M. Ristorini and S. Canepari, *Atmosphere*, 2019, **10**(12), DOI: 10.3390/atmos10120816.
16 A. Rengaraj, P. Puthiaraj, N. S. Heo, H. Lee, S. K. Hwang, S. Kwon, W. S. Ahn and Y. S. Huh, *Colloids Surf., B*, 2017, **160**, 1–10.
17 T. Miyazawa, T. Otomatsu, Y. Fukui, T. Yamada and S. Kuwata, *J. Chem. Soc., Chem. Commun.*, 1988, 419–420.
18 S. M. Mali, M. Ganesh Kumar, M. M. Katariya and H. N. Gopi, *Org. Biomol. Chem.*, 2014, **12**, 8462–8472.
19 T. Michels, R. Dölling, U. Haberkorn and W. Mier, *Org. Lett.*, 2012, **14**, 5218–5221.
20 P. Song, W. Du, W. Li, L. Zhu, W. Zhang, X. Gao, Y. Tao and F. Ge, *Nanomater. Nanotechnol.*, 2020, **10**, 1–10.
21 M. De Zotti, B. Biondi, Y. Park, K.-S. Hahm, M. Crisma, C. Toniolo and F. Formaggio, *Amino Acids*, 2012, **43**, 1761–1777.
22 Z. Zhai, K. Xu, L. Mei, C. Wu, J. Liu, Z. Liu, L. Wan and W. Zhong, *Soft Matter*, 2019, **15**, 8603–8610.
23 D. J. Tobin, *J. Tissue Viability*, 2017, **26**, 37–46.
24 M. Schieber and N. S. Chandel, *Curr. Biol.*, 2014, **24**, 453–462.

25 H. Choi, J. Park, H. Kim, D. Kim and S. Kim, *BMB Rep.*, 2009, **42**, 743–746.
26 R. K. Lane, T. Hilsabeck and S. L. Rea, *Biochim. Biophys. Acta, Bioenerg.*, 2015, **1847**, 1387–1400.
27 N. Tsuji, S. Moriwaki, Y. Suzuki, Y. Takema and G. Imokawa, *Photochem. Photobiol.*, 2001, **74**, 283–290.
28 J. Varani, M. K. Dame, L. Rittie, S. E. G. Fligiel, S. Kang, G. J. Fisher and J. J. Voorhees, *Am. J. Pathol.*, 2006, **168**, 1861–1868.
29 I. Valle, A. Álvarez-Barrientos, E. Arza, S. Lamas and M. Monsalve, *Cardiovasc. Res.*, 2005, **66**, 562–573.
30 L. Suchá, R. Šuláková, R. Fryčák and I. Dolečková, *Cosmetics*, 2018, **5**, 18.
31 R. Anderson and T. Prolla, *Biochim. Biophys. Acta*, 2009, **1790**, 1059–1066.
32 S. Austin and J. St-pierre, *J. Cell Sci.*, 2012, **125**, 4963–4971.